Petroleum Science 18 (2021) 1788–1796

Contents lists available at ScienceDirect

Petroleum Science

journal homepage: www.keaipublishing.com/en/journals/petroleum-science

Original Paper

Mechanism of CO_2 enhanced oil recovery in shale reservoirs

Hai-Bo Li [a, b], Zheng-Ming Yang [a, b, *], Rui-Shan Li [c], Ti-Yao Zhou [a], He-Kun Guo [a, b], Xue-Wei Liu [a, b], Yi-Xin Dai [d], Zhen-Guo Hu [c], Huan Meng [a]

[a] PetroChina Research Institute of Petroleum Exploration and Development, Beijing, 100083, PR China
[b] Institute of Flow and Fluid Mechanics, Chinese Academy of Sciences, Langfang, 065007, Hebei, PR China
[c] Sinopec Jianghan Oilfield Company Research Institute of Exploration and Development, Wuhan, 430223, Hubei, PR China
[d] University of Chinese Academy of Sciences, Beijing, 100049, PR China

ARTICLE INFO

Article history:
Received 23 June 2020
Accepted 16 April 2021
Available online 27 September 2021

Edited by Yan-Hua Sun

Keywords:
Shale oil
CO_2
Supercritical pressure
NMR
Core physical simulation
Slim-tube test
Component analysis
Nano-CT

ABSTRACT

Combined with NMR, core experiment, slim-tube tests, nano-CT and oil composition analysis, the mechanism of CO_2 enhanced oil recovery had been studied. CO_2 flooding under supercritical state could achieve higher oil recovery. In the process of crude oil displaced by supercritical CO_2, the average oil recovery was 46.98% at low displacement pressures and 73.35% at high displacement pressures. The permeability of cores after CO_2 flooding was only 28%–64% of those before flooding. As to the expelled oil, the contents of asphaltenes and non-hydrocarbons decreased, and saturated hydrocarbons of above C25 were absent in some samples, indicating that they had been retained in cores as demonstrated by CT and NMR experiments. In slim-tube tests, the heavy components of oil were expelled when the pressure increased to 30 MPa. There was a reasonable bottom hole pressure (BHP) below which the heavy components driven out from the far-well zone would deposit in the near-well zone, and when the pressure was too high, the nonhydrocarbon detention may cause block. The smaller throat and worse physical properties the porous media had, the higher displacement pressure would be required to achieve a good oil displacement efficiency. The increase in displacement pressure or time of interaction between oil and CO_2 could effectively enhance oil recovery.

1. Introduction

The successful development practices of shale oil in the United States have changed the global energy landscape (Jia et al., 2012; Zou et al., 2015). China has abundant shale oil reserves and great development potential (Guo et al., 2016; Wu et al., 2015, 2016; Yang et al., 2013; Zhang et al., 2016). A large number of scholars have studied the shale oil exploration potential evaluation, enrichment rules, geological characteristics, etc. (Liu et al., 2018; Yang et al., 2016, 2019, Zou et al., 2015). For low-permeability tight reservoirs, a large number of scholars have studied their pore structure, fluid occurrence and effective production (Bai et al., 2013; Feng et al., 2019; Li et al., 2015, 2016, 2018; Lin et al., 2019; Zhao et al., 2015; Yang et al., 2014; Yao et al., 2013). Zhang et al. (2018) Uth et al. (2016) and Dastvareh and Azaiez, 2017 studied liquid flow in nano- or micro-scale circular tubes. Wei et al. (2014) and Datta et al. (2014) studied the fluid flow mechanism from a three-dimensional porous medium. De Paoli et al. (2016), Yao et al. (2013) and Rokhforouz and Amiri (2017) studied the flow behavior of fluids in the heterogeneous porous media. Carbon dioxide flooding is an approach that many experts valued to enhance shale oil recovery (Alfarge et al., 2018; Burrows et al., 2020; Hejazi et al., 2017; Jia et al., 2020; Song et al., 2020; Wang and Sheng, 2017; Xu et al., 2020; Yang et al., 2019; Zhang et al., 2017, 2020; Zhu et al., 2020; Zou et al., 2017). However, there are few studies of the mechanism of shale oil development in different media. Some scholars used field data to analyze the dynamic characteristics and mobility of shale oil production. Gao et al. (2014) used field data to study the production characteristics and gas channeling of CO_2 immiscible flooding wells. Zhang et al. (2014) used a combination of experimental analysis and logging data to analyze the mobility of shale oil from the perspective of formation energy. Wang et al. (2019) used a variety of experimental methods to study the mechanism of shale oil occurrence. Lu et al. (2018) established a

* Corresponding author. PetroChina Research Institute of Petroleum Exploration and Development, Beijing, 100083, PR China.
E-mail address: yzhm69@petrochina.com.cn (Z.-M. Yang).

https://doi.org/10.1016/j.petsci.2021.09.040

grading evaluation standard and the lower limit of reservoir formation for shale oil reservoirs. Some scholars have studied the characteristics of the reaction between CO_2 and crude oil. Lobanov et al. (2018) studied the mass transfer between heavy oil and liquid CO_2 after they are mixed. Most of the studies of the mechanism of CO_2 flooding are limited to microscopic experiments. Zhou et al. (2015) combined slim-tube experiments with microscopic simulation experiments to analyze the reservoir blocking mechanism during CO_2 flooding. Hu et al. (2019) adopted microscopic models to study the factors affecting the effect of CO_2 flooding. Jin et al. (2016, 2017), and Torres et al. (2018) studied advancing carbon dioxide enhanced oil recovery in the Bakken Unconventional System. Hawthorne et al. (2020), Kurz et al. (2018), Sorensen et al. (2018) studied minimum miscibility pressures using CO_2, influence of organics on supercritical CO_2 migration and CO_2 injection potential for enhanced oil recovery in the Bakken Reservoirs. Burrows et al. (2020), Song et al. (2020) and Jia et al. (2020) studied main oil recovery mechanisms of natural gas and carbon dioxide in unconventional reservoirs. There is no case of combining nuclear magnetic resonance (NMR), component analysis, nano CT and other technologies to study the mechanism of CO_2 enhanced oil recovery of shale oil. Combined with NMR, thin tube experiment and oil component analysis, this study analyzes the properties of oil driven by carbon dioxide at different pressures, and studies the action mechanism between carbon dioxide and oil in porous media. Combined NMR, physical simulation, nano-CT and oil composition analysis, oil recovery mechanism at different pressures are studied, and the mechanism of blocking in CO_2 flooding is analyzed from different ways. Combined with the huff-n-puff experiments, method of enhanced oil recovery of CO_2 flooding is proposed.

2. Experimental

2.1. Experimental materials

In this study, 9 core samples were obtained from shale oil reservoir of Jianghan oilfield, Jianghan Basin. The gas porosity values of these 9 core samples ranged from 6.38% to 22.05%, with an average of 15.59%, and the their gas permeability values were $(0.0016–16.5) \times 10^{-3}$ μm^2, with an average of 2.45×10^{-3} μm^2 (see Table 1). The brine used, with a salinity of 300,000 mg/L was prepared according to the composition of the formation water taken from the target reservoir and it was filtered through a 0.4-μm filter before use. High-purity helium and high-purity nitrogen were used to measure core porosity and permeability, respectively. The oil used in the experiment is from Jianghan oilfield, with a density of 0.79 g/cm^3 and a viscosity of 2.95 mPa s.

2.2. NMR experimental principle

The transverse relaxation time of the fluid in pores of cores depends mainly on the magnitude of the force between the pore surface and the fluid molecules. When fluid molecules are subjected to a strong force on the surface of the pore solid (such as fluids in small pores or fluids in large pores which are in close contact with the pore surface), this portion of fluid exhibits a small transverse relaxation time on NMR spectrum. On the contrary, when fluid molecules are subjected to a weak force on the surface of pore (such as fluids that are not in close contact with the surface in larger pores), the transverse relaxation time of this part of fluid is large.

2.3. Experimental procedures

The NMR experiment was performed using a Reccore-04 Core NMR Analyzer. The NMR core measurement was based on the oil and gas industry standard SY/T 6490-2007. The CO_2 flooding and the huff-n-puff experiments were performed using the SL-2018 carbon dioxide core flooding system.

The experimental procedures for conducting CO_2 flooding in core samples are described as follows:

(1) The fresh core sample was firstly evacuated with a vacuum pump, and then saturated with kerosene for more than 12 h before being subjected to pressure saturation.
(2) The core sample was installed in the core flooding system. The experimental temperature was adjusted to 80 °C, and the core was displaced with crude oil until no oil was expelled.
(3) The core was weighed and carried out NMR T_2 spectrum test.
(4) The core was loaded into the CO_2 core experimental system and the inlet and outlet pressures of the core were controlled with a high pressure and high precision plunger pump and a back-pressure valve, respectively. The confining pressure was controlled with a manual pump. Under the condition of maintaining a constant confining pressure, CO_2 flooding experiment was then carried out. The core was displaced until no crude oil was produced and then the core was taken out from the experimental system.
(5) The core was weighed and then its NMR T_2 spectrum was measured.
(6) Steps (4)–(5) were repeated at different CO_2 flooding pressures.
(7) NMR T_2 spectra of the cores saturated with crude oil and under different displacement pressures were plotted and analyzed.
(8) Some typical cores after the displacement were selected to carry out nano-CT scanning, and initiated NMR and component analysis on the crude oil displaced with CO2 to study the mechanism of CO2 enhanced oil recovery.

Experimental procedures of slim-tube CO_2 flooding tests are described as follows:

(1) Slim-tubes were connected to the CO_2 experimental system, and then the system was evacuated. Simulated formation water was pumped into slim tubes with a high-pressure and high-precision plunger pump until the slim-tubes was completely saturated with water.
(2) The system temperature was set to 80 °C and water in the slim-tubes was displaced with crude oil to fill the slim-tubes with crude oil.
(3) The inlet pressure of the slim-tubes test increased to 12 MPa and the pressure difference between the inlet and outlet was about 0.5 MPa CO_2 flooding experiment was performed until no crude oil was produced.
(4) The inlet pressure gradually increased from 12 MPa to 30 MPa, and the pressure difference between the inlet and outlet was maintained at about 0.5 MPa. The slim-tubes was displaced at each pressure until no crude oil was produced.
(5) The crude oil was displaced at different pressures and the oil expelled from the tubes was collected with measuring cylinders and named in sequence.

Table 1
Physical properties of core samples obtained from shale oil reservoirs of Jianghan oilfield.

Core No.	Lithology	Length, cm	Diameter, cm	Gas porosity, %	Gas permeability, mD
1	Gypsum mudstone	5.90	2.45	19.85	0.25
2	Glauberite mudstone	5.26	2.45	22.05	0.34
3	Gypsum mudstone	5.59	2.45	20.40	0.33
4	Dolomitic mudstone	4.04	2.46	13.70	3.01
5	Dolomitic mudstone	4.92	2.48	13.90	16.50
6	Dolomitic mudstone	5.50	2.46	17.61	0.18
7	Lime mudstone	6.60	2.47	19.25	0.54
8	Argillaceous dolomite	4.82	2.53	6.38	0.00165
9	Glauberite mudstone	2.96	2.50	7.17	0.854

(6) The oil volume and weight were recorded separately.
(7) NMR spectra and composition of the crude oil expelled at different displacement pressures were analyzed to investigate the mechanism of CO_2 enhanced oil recovery.

3. Experimental results and discussion

3.1. Mechanism of CO_2 flooding in shale oil

In order to compare the shale oil recovery efficiencies by N_2 injection and CO_2 injection, respectively, and compare the oil recovery by conventional CO_2 injection (non-supercritical) and supercritical CO_2 injection, two series of core flooding tests were carried out. The experimental data is shown in Table 2.

After the core sample was saturated with kerosene, N_2 was injected into the core sample at an injection pressure of 5 MPa (NMR was carried out before and after N_2 displacement), and then the core sample was dried and re-saturated with kerosene to carry out CO_2 displacement test (the experimental procedures are as described in Section 2.3). Comparisons of T_2 spectra of two core samples before and after N_2 and CO_2 displacement are shown in Figs. 1 and 2. It can be seen from Fig. 1 and Table 2 that at a displacement pressure of 5 MPa, both N_2 flooding and CO_2 flooding had low recoveries of 6.02% and 11.45%, respectively for No. 8 core sample, indicating that under low displacement pressure, CO_2 flooding could not achieve a high displacement efficiency and had no obvious advantage over N_2 flooding. In No. 9 core sample, at a displacement pressure of 5 MPa the oil recoveries were 7.48% by N_2 flooding and 8.88% by CO_2 flooding, respectively; while at a high displacement pressure of 16 MPa the oil recovery by CO_2 flooding was 41.22%, which shows that in the supercritical condition (the critical temperature of CO_2 is 31.26 °C, and the critical pressure is 7.29 MPa), CO_2 flooding can achieve a high displacement recovery, which has obvious advantages over non supercritical N_2 and CO_2 flooding.

The supercritical CO_2 flooding experiments were performed on 7 core samples and experimental results are shown in Table 3. The T_2 spectra of partial core samples before and after flooding are shown in Fig. 3. The group components of the oil expelled from some core samples are shown in Table 4. The comparison of the components of the oil expelled from No. 3 core sample and the crude oil is shown in Fig. 4.

It could be seen from Table 3 and Fig. 3 that the CO_2 under supercritical state had a high flooding recovery ratio. The sweep efficiencies of the 7 samples under lower displacement pressure were relatively high, ranging from 26.12% to 69.29%, with an average of 46.98.%. The flooding recovery ratios of the samples under high displacement pressures were high, ranging from 48.51% to 93.46%, with an average of 73.35%. Low-pressure CO_2 displacement test was not carried out on No. 3 core sample; and the high-pressure displacement test was performed at 19.29 MPa and achieved an extremely high flooding recovery, reaching 93.46%.

The components of the oil expelled from the core samples by CO_2 flooding were shown in Table 4 and Fig. 4. The asphaltenes (heptanes-insoluble) were generally reduced, and the non-hydrocarbons were partially reduced. In some samples, the components above the C20 were absent. Taking No. 3 core sample as an example, the contents of asphaltenes and non-hydrocarbons were both low (1.58% and 10.51%, respectively), and the heavy components above C20 were absent, indicating that a large amount of asphaltenes, non-hydrocarbons and saturated hydrocarbons above C20 had been retained in the core samples. Hawthorne et al. (2018) studied the variations in the molecular weight of oil (or oil composition) with pressure, which might support the findings in this study.

Fig. 5 shows the permeability comparison of No. 1, No. 2 and No. 7 core samples before and after displacement. It could be seen from the figure that the permeability of the core samples after displacement was only 28%–64% of those before displacement, indicating that the core samples had been clogged severely after displacement.

Fig. 6 shows CT scans of No. 3 and No. 42 core samples after CO_2 and N_2 flooding, respectively. No. 3 core sample was saturated with crude oil for CO_2 flooding, and No. 42 core sample was saturated with kerosene for N_2 flooding. It could be seen from the figure that after the high-pressure displacement by CO_2, the remaining oil in the core sample mainly occurred in the form of isolated oil, micro-fractured films and clusters. Among them, the residual oil film on the surface of the micro-fractures had a large thickness, which had major blocking effect on the micro-fractures and reduced the core permeability. The remaining oil porosity of No. 3 and No. 42 core samples were 0.61% and 0.15%, respectively, which indicated that there was heavy component deposition after CO_2 flooding crude oil, resulting in the remaining oil percentage on macroporous surfaces

Table 2
A comparison of oil displacement between CO_2 and N_2 flooding in shale oil core samples.

Core No.	N_2 flooding			CO_2 flooding		
	Inlet pressure, MPa	Outlet pressure, MPa	Flooding recovery, %	Inlet pressure, MPa	Outlet pressure, MPa	Flooding recovery, %
8	5.00	0	6.02	5.00	0	11.45
9	5.00	0	7.48	5.00	4.00	8.88
9	/	/	/	16.30	16.00	41.22

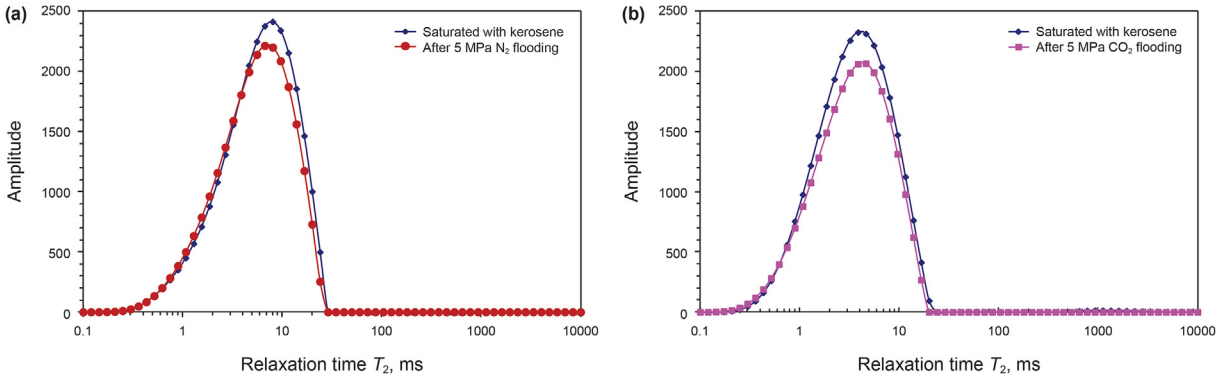

Fig. 1. T_2 spectra before and after N_2 flooding (**a**) and CO_2 flooding (**b**) in No. 8 core sample.

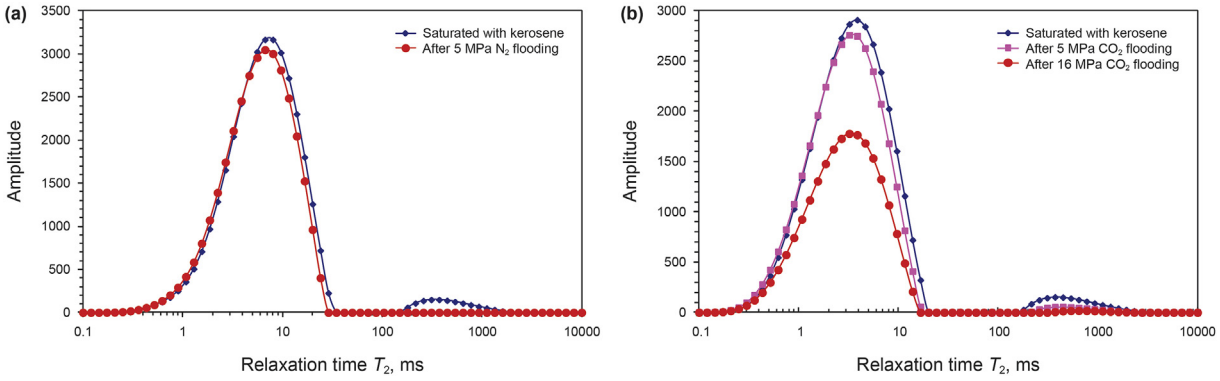

Fig. 2. T_2 spectra before and after N_2 flooding (**a**) and CO_2 flooding (**b**) in No. 9 core sample.

Table 3
CO_2 flooding data of 7 shale oil cores.

Core No.	Low-pressure CO_2 flooding			High-pressure CO_2 flooding		
	Inlet pressure, MPa	Outlet pressure, MPa	Flooding recovery, %	Inlet pressure, MPa	Outlet pressure, MPa	Flooding recovery, %
1	14.20	7.00	69.29	19.32	14.71	88.26
2	8.20	6.70	54.83	19.31	11.58	80.27
3	/	/	/	19.29	16.50	93.46
4	10.25	7.76	27.57	19.28	15.29	63.22
5	10.00	10.00	26.12	17.79	17.79	48.51
6	12.15	6.60	57.24	19.31	13.67	71.97
7	15.09	7.02	46.81	21.04	12.63	67.76

much higher than that of N_2 flooding kerosene. From the T_2 spectra before and after core displacement, the small relaxation time parts of the T_2 spectra after flooding for some core samples were significantly higher than those before the flooding (No. 1 and No. 2 core samples in Fig. 3), which could also indirectly explain the deposition of heavy components on the surface of the pore throats.

The analysis of the composition of the oil after CO_2 flooding indicates that under the low-pressure and high-pressure displacement, the asphaltenes of the oil were generally reduced. When the displacement pressure was higher than a certain value, the non-hydrocarbons of the oil would be reduced, while the proportion of saturated hydrocarbons having a large molecular weight would be increased. The reservoir engineering and actual production had confirmed that the reservoir pressure drop was spatially funnel-shaped, and the closer it was to the oil well, the lower pressure and the greater pressure drop the reservoir have. Regardless of the high-pressure zone far from the well or the low-pressure zone near the well, there would be asphaltene deposits; there was a reasonable bottom hole pressure (BHP), below which the high molecular weight saturated hydrocarbons driven out of the zone far from the well would be deposited in the zone near the well, which caused blockage; when the production pressure was too high, it would cause a large amount of non-hydrocarbon retention, leading to reservoir blockage.

3.2. Slim-tube experiment analysis

In order to study the properties of the oil expelled by CO_2 under different pressures, and further compare interaction mechanism between CO_2 and oil in porous media with different permeability, slim-tube experiments were carried out (the slim tube is a sand-filled model, which is 20 m long with large pore throat size and high permeability, and the water measured permeability is 38 mD), and then NMR and component analysis were performed on some oil samples expelled from the slim tube. In the slim-tube experiment, the crude oil displaced by different pressures of CO_2 was

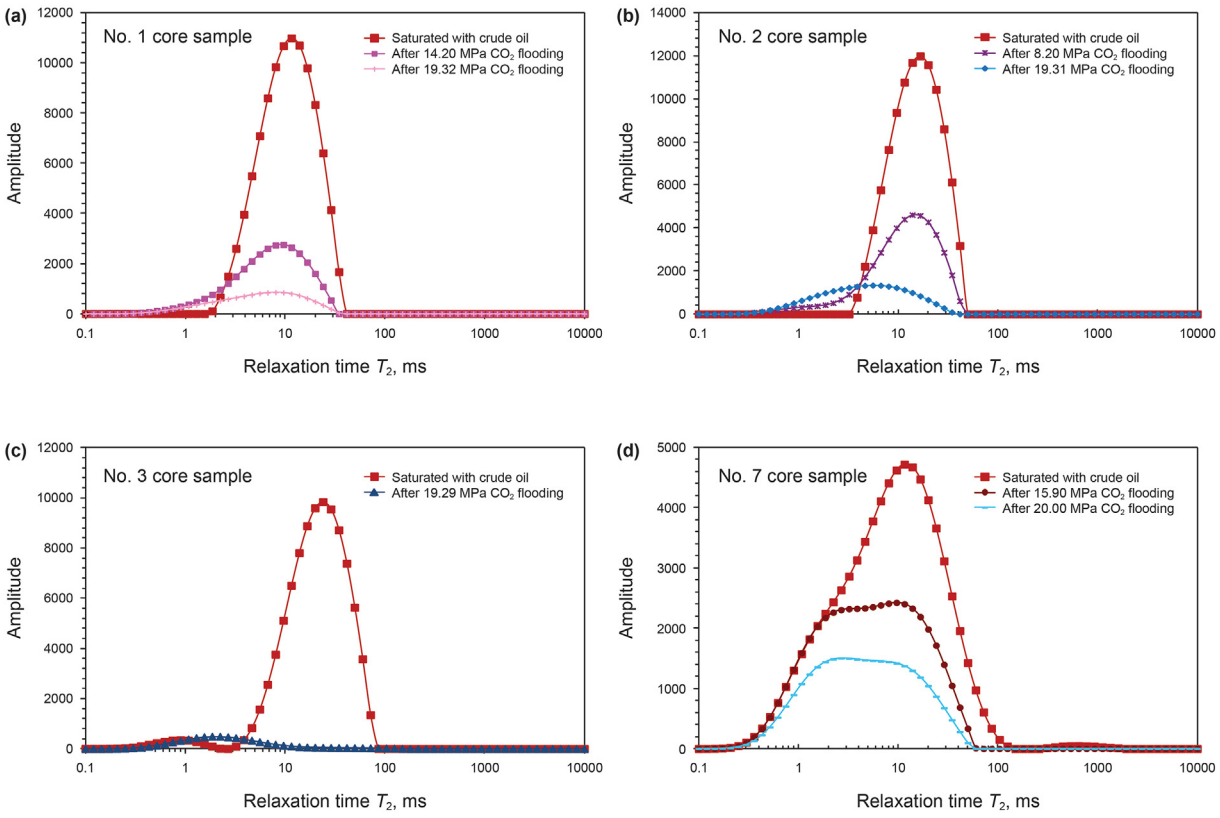

Fig. 3. T_2 spectra of core samples before and after CO_2 flooding.

Table 4
Group components of crude oil expelled from core samples.

Oil sample No.	Group component, %			
	Saturated hydrocarbons	Aromatic hydrocarbons	Nonhydrocarbons	Asphaltenes
Y0	45.76	19.39	30.71	4.14
Y1	49.45	20.44	28.10	2.01
Y3	74.96	12.95	10.51	1.58
Y6	49.09	19.57	29.35	1.99
Y7	49.17	18.08	30.14	2.61

Note: Y0 represents crude oil sample; Y1, Y3, Y6 and Y7 represent crude oil samples expelled from No. 1, 3, 6, and 7 core samples, respectively.

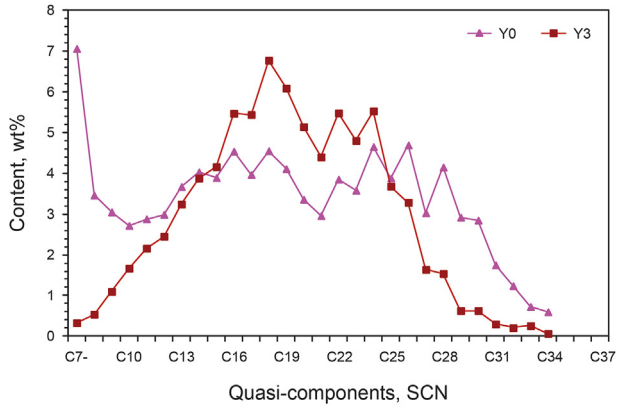

Fig. 4. Component concentrations of the crude oil (Y0) and the oil (Y3) expelled from No. 3 core sample with CO_2 flooding.

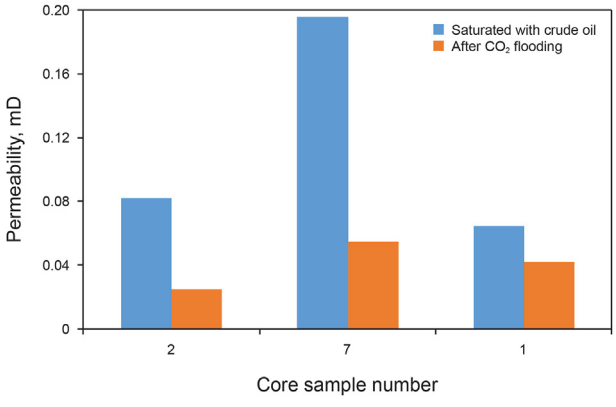

Fig. 5. Comparison of permeability of three core samples before and after CO_2 displacement.

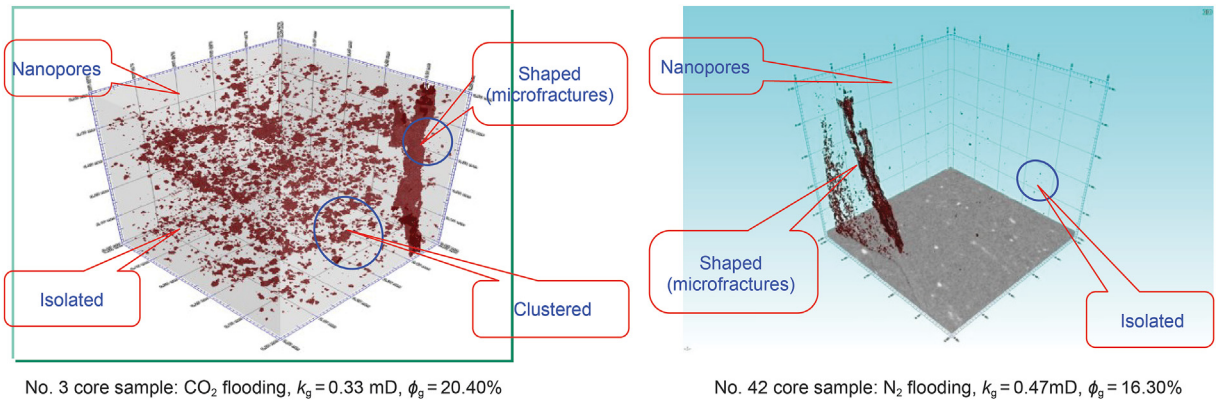

Fig. 6. CT scans of No. 3 and No. 42 core samples after CO_2 and N_2 flooding.

collected in measuring cylinders, and the cylinders were numbered as shown in Fig. 7. In order to study the components of the oil, the oil in each cylinder was tested by NMR. The T_2 spectra comparison of crude oil and oil in No. 2, No. 6, No.10, No.11, and No. 14 cylinders is shown in Fig. 8. This study also carried out quasi-component analysis on oil samples in No. 2, No. 6, No. 7, and No. 14 cylinders (Fig. 9). Table 5 shows the distribution of the group compositions of oil samples in four measuring cylinders (No. 2, No. 6, No. 7, and No. 14). The oil samples in No. 2, No. 6 and No. 7 measuring cylinders were respectively collected at the early, late and last displacement stage at the displacement pressure of 12 MPa. The oil samples in 9–13 measuring cylinders were expelled from the slim-tube experiments at 13, 16, 20, 21 and 24 MPa, respectively. Because the amount of oil expelled in this pressure range (13–24 MPa) was very small and a certain amount of water was expelled, the oil-water mixture stored in the measuring cylinder was unable to be analyzed for the oil components.

It can be seen from Figs. 7–9 and Table 5 that, the slim-tube had a large throat size and high permeability than shale cores; before gas appears in 12 MPa displacement process, the amount of oil expelled was more than 80%, which indicated that the pore structure and density of the porous media also had a significant impact on the CO_2 displacement effect. The smaller pore throat and the lower permeability porous media had, the higher the displacement pressure would be needed to achieve better oil displacement effect. The quasi-components of the crude oil and the oil in No. 2 and No. 6 measuring cylinders were same, and the T_2 spectra of crude oil, oil

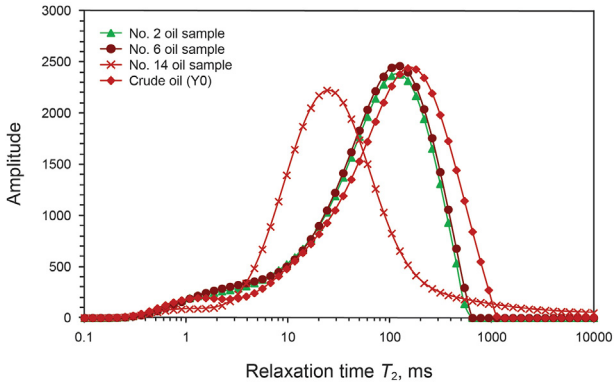

Fig. 8. Comparison of T_2 spectra of crude oil and the oil samples expelled at different pressures.

in No. 2 and No. 6 measuring cylinders were the same, indicating that the oil properties were the same. When the pressure had increased from 13 to 24 MPa, the amount of the expelled oil was small. When the pressure had increased to 30 MPa, the T_2 spectrum of No. 14 oil sample was shifted to the left. In the quasi-component analysis, the oil expelled was mainly composed of C20 to C34 heavy components. In the group component analysis, the contents of non-hydrocarbons and asphaltenes were significantly lower than those of the oil sample displaced at a pressure of 12 MPa, indicating that a

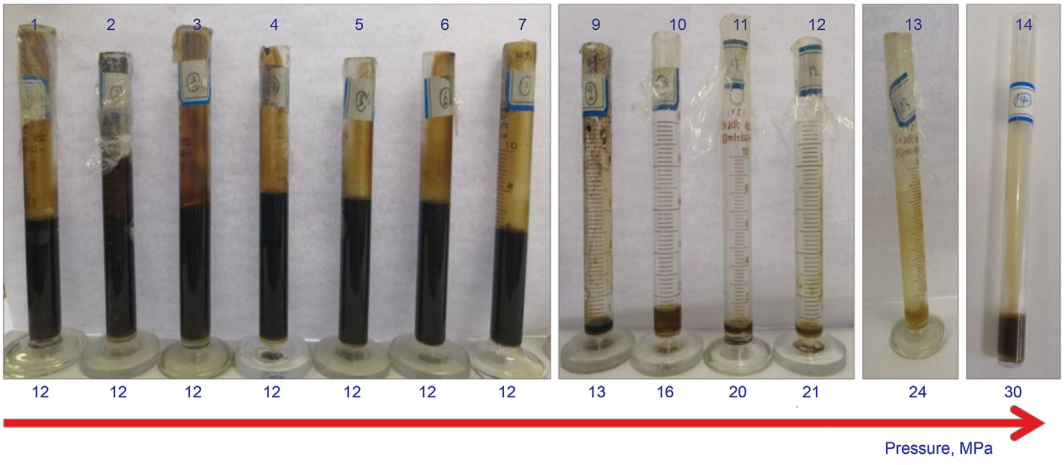

Fig. 7. Oil samples expelled from slim-tubes by CO_2 flooding.

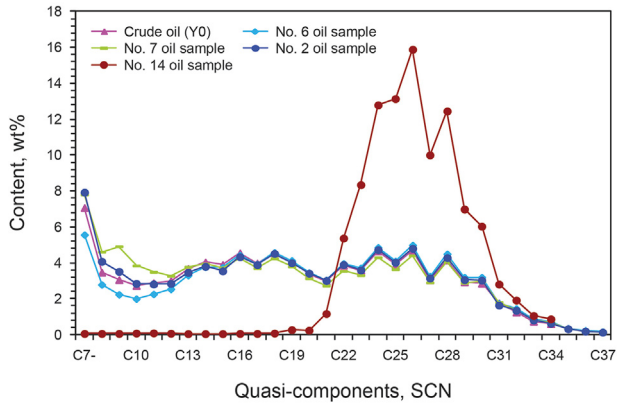

Fig. 9. Comparison of quasi-components of crude oil and oil samples expelled at different pressures.

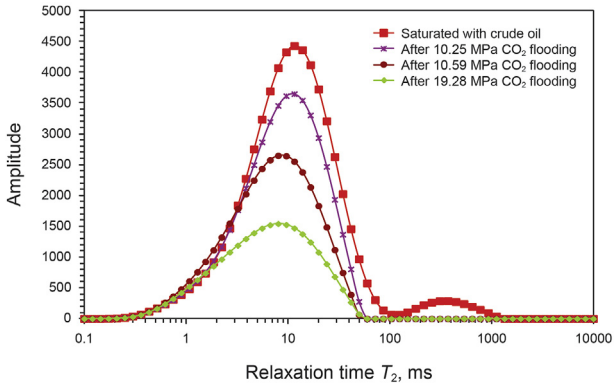

Fig. 10. Comparison of T_2 spectra of No. 4 core sample at different displacement pressures.

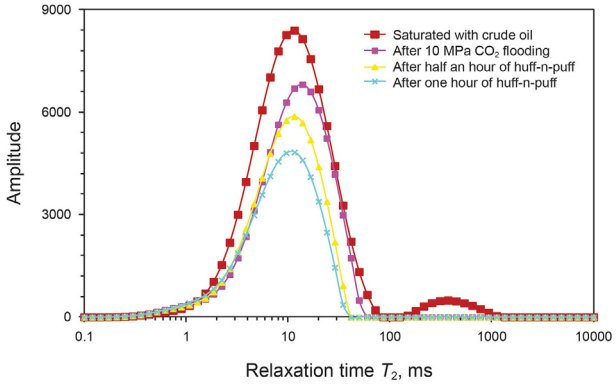

Fig. 11. Comparison of T_2 spectra of different huff-n-puff stages of No.5 core sample.

large-amount of non-hydrocarbons and asphaltenes had been retained in the slim-tubes at this pressure.

It could be seen from Table 5 that the asphaltene contents in No. 2, 6, 7, and 14 oil samples reduced, indicating that CO_2 flooding could not displace all asphaltenes, and some asphaltenes had been retained in the slim-tubes after displacement.

3.3. Methods of enhanced CO_2 flooding

As can be seen from the foregoing, the increase in CO_2 displacement pressure could effectively improve the oil recovery. Fig. 10 shows the comparison of T_2 spectra of No. 4 core samples at different displacement pressures (when the pressures at the inlet and outlet of No. 4 core sample were increased, the oil recovery increased from 42% to 63%). The slim-tube model had high permeability and large pore throat size, and micro-throats was the main throat, from which crude oil could be driven out at low displacement pressure (12 MPa). The matrix of shale oil core sample was tight, and the throats in the sale core were mainly submicron- and nanometer-sized. The density of supercritical CO_2 increased with the increasing displacement pressure, and the ability of CO_2 to dissolve and extract oil enhanced; on the other hand, the increasing density of supercritical CO_2 could make CO_2 more easily enter into the micro pore throats, and increase the volume of contacting oil; thus, the displacement recovery of CO_2 was improved.

The CO_2 huff-n-puff experiment was carried out using No. 5 dolomitic mudstone rock sample. The NMR test was carried out at different stages of the experiment (Fig. 11). The selected core contained fractures obviously. After the first CO_2 displacement stages, due to the influence of fractures, the matrix was not completely affected, and the flooding recovery was not high (only 26.1%). The outlet back pressure was controlled, and the flooding was carried out after half an hour of "soaking", and the oil recovery was then increased to 39%. After 2 h of "soaking" again, the oil recovery reached 48.5%. It can be seen that, due to the compactness of shale oil matrix, the complete interaction between CO_2 and crude oil takes longer. Increasing the interaction time between crude oil and CO_2 with CO_2 huff-n-puff could effectively improve the oil recovery.

4. Conclusions

Under supercritical state, CO_2 flooding could achieve a high oil displacement recovery, and had obvious advantages compared with non-supercritical N_2 and CO_2 flooding. In the process of supercritical CO_2 flooding experiments performed on crude oil-saturated cores, the average oil recovery of the six samples at relatively low displacement pressures (9.56 MPa) was 46.98%, and the average oil recovery of the seven samples at high displacement pressures (16.95 MPa) was 73.35%. When the CO_2 flooding was carried out at a high displacement pressure (19 MPa), the oil recovery was high (93%). The permeability of core samples after CO_2 flooding were only 28%–64% of those before flooding, and the

Table 5
Comparison of the group compositions of crude oil and oil samples expelled at different pressures.

Oil sample No.	Group composition, %				Corresponding displacement pressure, MPa
	Saturated hydrocarbons	Aromatic hydrocarbons	Nonhydrocarbons	Asphaltenes	
Crude oil (Y0)	45.76	19.39	30.71	4.14	/
2	44.76	19.92	31.24	4.08	12
6	45.71	19.96	30.44	3.89	12
7	44.87	19.20	32.32	3.61	12
14	74.61	18.76	3.66	2.97	30

reservoir blockage was serious. As to the expelled oil, asphaltenes generally decreased, and non-hydrocarbon partly decreased. As to some samples under high back pressure, saturated hydrocarbons of above C25 were missing, indicating that they had been retained in the core samples. The nano-CT spectra and T_2 spectra before and after core flooding also indicated that heavy components were adsorbed on surface of pore throats, resulting in a decrease in permeability the core sample. In the slim-tube tests, before gas appears in 12 MPa displacement process, the volume of the expelled oil was large, and the oil expelled in different stages had similar properties; when the pressure increased to 13–24 MPa, the amount of oil expelled at this pressure range was very small; when the pressure increased to 30 MPa, heavy components of oil was expelled. The oil expelled at 30 MPa was mainly heavy components of C20–C34, and the contents of asphaltenes and non-hydrocarbons had declined. There was a reasonable bottom hole pressure (BHP) below which the heavy components driven out from the far-well zone would be deposited in the near-well zone. However, when the BHP was too high, nonhydrocarbon detention may cause blocking. The smaller the pore throats and the worse physical properties the porous media had, the higher displacement pressure would be needed to achieve a good oil displacement effect. Increasing displacement pressure or time of interaction between crude oil and CO_2 could effectively enhance oil recovery.

Acknowledgments

We gratefully acknowledge financial support from the National Science and Technology Major Project (2017ZX05013-001, 2017ZX05069003, 2017ZX05049005-004) and Ministry of Science and Technology of PetroChina (2021ZZ01-03, kt2021-09-05, 2021DJ1806, 2017E-1514, 2018E-11-05).

References

Alfarge, D., Wei, M., Bai, B., 2018. CO_2-EOR mechanisms in huff-n-puff operations in shale oil reservoirs based on history matching results. Fuel 226, 112–120. https://doi.org/10.1016/j.fuel.2018.04.012.

Bai, B., Zhu, R., Wu, S., et al., 2013. Multi-scale method of nano(micro)-CT study on microscopic pore structure of tight sandstone. Petrol. Explor. Dev. 40 (3), 329–331. https://doi.org/10.1016/S1876-3804(13)60042-7.

Burrows, L.C., Haeri, F., Cvetic, P., et al., 2020. A literature review of CO_2, natural gas, and water-based fluids for enhanced oil recovery in unconventional reservoirs. Energy Fuel. 34, 5331–5380. https://doi.org/10.1021/acs.energyfuels.9b03658.

Dastvareh, B., Azaiez, J., 2017. Instabilities of nanofluid flow displacements in porous media. Phys. Fluids 29 (7), 079901. https://doi.org/10.1063/1.4991753.

Datta, S.S., Ramakrishnan, T.S., Weitz, D.A., 2014. Mobilization of a trapped non-wetting fluid from a three-dimensional porous medium. Phys. Fluids 26 (2), 3. https://doi.org/10.1063/1.4866641.

De Paoli, M., Zonta, F., Soldati, A., 2016. Influence of anisotropic permeability on convection in porous media: implications for geological CO_2 sequestration. Phys. Fluids 28 (5), 056601. https://doi.org/10.1063/1.4947425.

Feng, J., Zhang, B., Feng, Z., et al., 2019. Crude oil mobility and its controlling factors in tight sand reservoirs in northern Songliao Basin, China. Petrol. Explor. Dev. 46 (2), 312–321. https://doi.org/10.1016/S1876-3804(19)60012-1.

Gao, Y., Zhao, M., Wang, J., et al., 2014. Performance and gas breakthrough during CO_2 immiscible flooding in ultra-low permeability reservoirs. Petrol. Explor. Dev. 41 (1), 79–85. https://doi.org/10.11698/PED.2014.01.10.

Guo, Y., Yan, S., Pang, X., et al., 2016. Characteristics and genetic mechanism of near source accumulated accumulation for continuous type tight sand gas. Earth Sci. 41 (3), 433–440. https://doi.org/10.3799/dqkx.2016.035 (in Chinese).

Hawthorne, S.B., Miller, D.J., Grabanski, C.B., et al., 2020. Experimental determinations of minimum miscibility pressures using hydrocarbon gases and CO_2 for crude oils from the Bakken and Cut Bank Oil Reservoirs. Energy Fuel. 34 (5), 6148–6157. https://doi.org/10.1021/acs.energyfuels.0c00570.

Hawthorne, S.B., Miller, D.J., Jin, L., et al., 2018. Lab and reservoir study of produced hydrocarbon molecular weight selectivity during CO_2 enhanced oil recovery. Energy Fuel. 32 (9), 9070–9080. https://doi.org/10.1021/acs.energyfuels.8b01645.

Hejazi, S.H., Assef, Y., Tavallali, M., et al., 2017. Cyclic CO_2-EOR in the Bakken Formation: variable cycle sizes and coupled reservoir response effects. Fuel 210 (15), 758–767. https://doi.org/10.1016/j.fuel.2017.08.084.

Hu, Y., Hao, M., Chen, G., et al., 2019. Technologies and practice of CO_2 flooding and sequestration in China. Petrol. Explor. Dev. 46 (4), 716–727. https://doi.org/10.11698/PED.2019.04.10.

Jia, C., Zou, C., Li, J., et al., 2012. Assessment criteria, main types, basic features and resource prospects of the tight oil in China. Acta Pet. Sin. 33 (3), 343–350. https://doi.org/10.1016/0031-9384(73)90235-7.

Jin, L., Hawthorne, S., Sorensen, J., et al., 2017. Advancing CO_2 enhanced oil recovery and storage in unconventional oil play-Experimental studies on Bakken shales. Appl. Energy 208 (15), 171–183. https://doi.org/10.1016/j.apenergy.2017.10.054.

Jin, L., Sorensen, J., Hawthorne, S., et al., 2016. Improving oil recovery by use of carbon dioxide in the Bakken Unconventional System: a laboratory investigation. SPE Reservoir Eval. Eng. 20 (3), 602–612. https://doi.org/10.2118/178948-PA.

Kurz, B.A., Sorensen, J.A., Hawthorne, S.B., et al., 2018. The influence of organics on supercritical CO_2 migration in organic-rich shales. Unconventional Resources Technology Conference, Texas, USA, doi:10.15530/urtec-2018-2902743.

Li, D., Zha, W., Liu, S., et al., 2016. Pressure transient analysis of low permeability reservoir with pseudo threshold pressure gradient. J. Petrol. Sci. Eng. 147, 308–316. https://doi.org/10.1016/j.petrol.2016.05.036.

Li, H., Guo, H., Yang, Z., et al., 2015. Tight oil occurrence space of triassic chang 7 layer in northern shaanxi area, erdos basin. Petrol. Explor. Dev. 42 (3), 396–400. https://doi.org/10.1016/S1876-3804(15)30036-7.

Li, W., Li, X., Yang, Z., et al., 2018. A new improved threshold segmentation method for scanning images of reservoir rocks considering pore fractal characteristics. Fractals 26 (2), 1840003. https://doi.org/10.1142/S0218348X1 8400030.

Lin, W., Li, X., Yang, Z., et al., 2019. Multiscale digital porous rock reconstruction using template matching. Water Resour. Res. 55 (8), 6911–6922. https://doi.org/10.1029/2019WR025219.

Liu, B., Shi, J., Fu, X., et al., 2018. Petrological characteristics and shale oil enrichment of lacustrine fine-grained sedimentary system: a case study of organic-rich shale in first member of Cretaceous Qingshankou Formation in Gulong Sag, Songliao Basin, NE China. Petrol. Explor. Dev. 45 (5), 828–837. https://doi.org/10.1016/S1876-3804(18)30091-0.

Lobanov, A.A., Shhekoldin, K.A., Struchkov, I.A., et al., 2018. Swelling and extraction test of heavy oil in a Russian reservoir by liquid carbon dioxide. Petrol. Explor. Dev. 45 (5), 861–868. https://doi.org/10.1016/S1876-3804(18)30095-8.

Lu, S., Li, J., Zhang, P., et al., 2018. Classification of microscopic pore-throats and the grading evaluation on shale oil reservoirs. Petrol. Explor. Dev. 45 (3), 436–444. https://doi.org/10.1016/S1876-3804(18)30050-8.

Rokhforouz, M.R., Amiri, H.A., 2017. Phase-field simulation of counter-current spontaneous imbibition in a fractured heterogeneous. porous medium. Phys. Fluids 29 (6), 2286. https://doi.org/10.1063/1.4985290, 146.

Song, Z., Song, Y., Li, Y., et al., 2020. A critical review of CO_2 enhanced oil recovery in tight oil reservoirs of North America and China. Fuel 276, 118006. https://doi.org/10.1016/j.fuel.2020.118006.

Sorensen, J.A., Pekot, L.J., José, A., et al., 2018. Field test of CO_2 injection in a vertical Middle Bakken Well to evaluate the potential for enhanced oil recovery and CO_2 storage. Unconventional Resources Technology Conference, Texas, USA. https://doi.org/10.15530/urtec-2018-2902813.

Torres, J.A., Jin, L., Bosshart, N.W., et al., 2018. Multiscale modeling to evaluate the mechanisms controlling CO_2-based enhanced oil recovery and CO_2 storage in the Bakken Formation. SPE/AAPG/SEG Unconventional Resources Technology Conference, Texas, USA, doi:10.15530/urtec-2018-2902837.

Uth, M.F., Jin, Y., Kuznetsov, A.V., et al., 2016. A direct numerical simulation study on the possibility of macroscopic turbulence in porous media: effects of different solid matrix geometries, solid boundaries, and two porosity scales. Phys. Fluids 28 (6), 70–77. https://doi.org/10.1063/1.4949549.

Wang, M., Ma, R., Li, J., et al., 2019. Occurrence mechanism of lacustrine shale oil in the paleogene shahejie formation of jiyang depression, bohai bay basin, China. Petrol. Explor. Dev. 46 (4), 789–802. https://doi.org/10.1016/S1876-3804(19)60242-9.

Wang, X., Sheng, J.J., 2017. Effect of low-velocity non-Darcy flow on well production performance in shale and tight oil reservoirs. Fuel 190, 41–46. https://doi.org/10.1016/j.fuel.2016.11.040.

Wei, X., Ok, J.T., Feng, X., et al., 2014. Effect of pore geometry and interfacial tension on water-oil displacement efficiency in oil-wet microfluidic porous media analogs. Phys. Fluids 26 (9), 093102. https://doi.org/10.1063/1.4894071.

Wu, G., Fang, H., Han, Z., et al., 2016. Growth features of measured oil initially in place & gas initially in place during the 12th Five-Year Plan and its outlook for the 13th Five-Year Plan in China. Acta Pet. Sin. 37 (9), 1145–1151. https://doi.org/10.7623/syxb201609008 (in Chinese).

Wu, S., Zou, C., Zhu, R., et al., 2015. Reservoir quality characterization of upper triassic chang 7 shale in ordos basin. Earth Sci. J. China Univ. Geosci. 11, 1810–1823. https://doi.org/10.3799/dqkx.2015.162 (in Chinese).

Xu, Z.X., Li, S.Y., Li, B.F., et al., 2020. A review of development methods and EOR technologies for carbonate reservoirs. Petrol. Sci. 17 (4), 990–1013. https://doi.org/10.1007/s12182-020-00467-5.

Yang, H., Li, S., Liu, X., 2013. Characteristics and resource prospects of tight oil and shall oil in Ordos Basin. Acta Pet. Sin. 34 (1), 1–11. https://doi.org/10.7623/syxb201301001 (in Chinese).

Yang, H., Niu, X., Xu, L., et al., 2016. Exploration potential of shale oil in Chang7 member, upper triassic yanchang formation, ordos basin, NW China. Petrol. Explor. Dev. 43 (4), 511–520. https://doi.org/10.1016/S1876-3804(16)30066-0.

Yang, W., Zhu, Y., Chen, S., et al., 2014. Characteristics of the nanoscale pore structure in Northwestern Hunan shale gas reservoirs using field emission scanning electron microscopy, high-pressure mercury intrusion, and gas adsorption. Energy Fuels 28 (2), 945–955. https://doi.org/10.1021/ef402159e.

Yang, Z.L., Yu, H.Y., Chen, Z.W., et al., 2019. A compositional model for CO_2 flooding including CO_2 equilibria between water and oil using the Peng–Robinson equation of state with the Wong–Sandler mixing rule. Petrol. Sci. 17, 874–889 (in Chinese), CNKI:SUN:SYKX.0.2019-04-012.

Yao, J., Deng, X., Zhao, Y., et al., 2013. Characteristics of tight oil in triassic yanchang formation, ordos basin. Petrol. Explor. Dev. 40 (2), 150–158. https://doi.org/10.1016/S1876-3804(13)60019-1.

Zhang, L., Bao, Y., Li, J., et al., 2014. Movability of lacustrine shale oil: a case study of dongying sag, jiyang depression, bohai bay basin. Petrol. Explor. Dev. 41 (6), 703–711. https://doi.org/10.1016/S1876-3804(14)60084-7.

Zhang, M., Zhan, S., Jin, Z., 2020. Recovery mechanisms of hydrocarbon mixtures in organic and inorganic nanopores during pressure drawdown and CO_2 injection from molecular perspectives. Chem. Eng. J. 382, 122808. https://doi.org/10.1016/j.cej.2019.122808.

Zhang, X., Zhu, W., Cai, Q., et al., 2018. Compressible liquid flow in nano- or micro-sized circular tubes considering wall–liquid Lifshitz–van der Waals interaction. Phys. Fluids 30 (6), 062002. https://doi.org/10.1063/1.5023291.

Zhang, X.S., Wang, H.J., Ma, F., et al., 2016. Classification and characteristics of tight oil plays. Petrol. Sci. 13 (1), 18–33. https://doi.org/10.1007/s12182-015-0075-0.

Zhang, Y., Lashgari, H.R., Di, Y., et al., 2017. Capillary pressure effect on phase behavior of CO_2/hydrocarbons in unconventional reservoirs. Fuel 197, 575–582. https://doi.org/10.1016/j.fuel.2017.02.021.

Zhao, H., Ning, Z., Wang, Q., et al., 2015. Petrophysical characterization of tight oil reservoirs using pressure-controlled porosimetry combined with rate-controlled porosimetry. Fuel 154, 233–242. https://doi.org/10.1016/j.fuel.2015.03.085.

Zhou, T., Liu, X., Yang, Z., et al., 2015. Experimental analysis on reservoir blockage mechanism for CO_2 flooding. Petrol. Explor. Dev. 42 (4), 548–553. https://doi.org/10.1016/S1876-3804(15)30048-3.

Zhu, C.F., Guo, W., Wang, Y.P., et al., 2020. Experimental study of enhanced oil recovery by CO_2 huff-n-puff in shales and tight sandstones with fracture. Petrol. Sci. 17 (5), 1–18. https://doi.org/10.1007/s12182-020-00538-7.

Zou, C., Ding, Y., Lu, Y., et al., 2017. Concept, technology and practice of “man-made reservoirs.”. Petrol. Explor. Dev. 44 (1), 146–158. https://doi.org/10.1016/S1876-3804(17)30019-8.

Zou, C., Zhai, G., Zhang, G., et al., 2015. Formation, distribution, potential and prediction of global conventional and unconventional hydrocarbon resources. Petrol. Explor. Dev. 42 (1), 14–28. https://doi.org/10.1016/S1876-3804(15)60002-7.